



# Refinement of the Manufacturing Route and Evaluation of the Reinforcement Effect of MAX Phases in Al Alloy Matrix Composite Materials

A. Dmitruk<sup>a,\*</sup> , K. Naplocha<sup>a</sup> , A. Żak<sup>b</sup> , A. Strojny-Nędzka<sup>c</sup>

<sup>a</sup> Wrocław University of Science and Technology, Faculty of Mechanical Engineering, Department of Lightweight Elements Engineering, Foundry and Automation, Poland

<sup>b</sup> Wrocław University of Science and Technology, Faculty of Chemistry, Institute of Advanced Materials, Poland

<sup>c</sup> Łukasiewicz Institute of Microelectronics and Photonics, Poland

\* Corresponding author: E-mail address: anna.dmitruk@pwr.edu.pl

Received 24.10.2023; accepted in revised form 06.02.2024; available online 21.03.2024

## Abstract

Microwave Assisted Self-propagating High-temperature Synthesis (MASHS) was used to prepare open-porous MAX phase preforms in Ti-Al-C and Ti-Si-C systems, which were further used as reinforcements for Al-Si matrix composite materials. The pretreatment of substrates was investigated to obtain open-porous cellular structures. Squeeze casting infiltration was chosen to be implemented as a method of composites manufacturing. Process parameters were adjusted in order to avoid oxidation during infiltration and to ensure the proper filling. Obtained materials were reproducible, well saturated and dense, without significant residual porosity or undesired interactions between the constituents. Based on this and the previous work of the authors, the reinforcement effect was characterized and compared for both systems. For the Al-Si+Ti-Al-C composite, an approx. 4-fold increase in hardness and instrumental Young's modulus was observed in relation to the matrix material. Compared to the matrix, Al-Si+Ti-Si-C composite improved more than 5-fold in hardness and almost 6-fold in Young's modulus. Wear resistance (established for different loads: 0.1, 0.2 and 0.5 MPa) for Al-Si+Ti-Al-C was two times higher than for the sole matrix, while for Al-Si+Ti-Si-C the improvement was up to 32%. Both composite materials exhibited approximately two times lower thermal expansion coefficients than the matrix, resulting in enhanced dimensional stability.

**Keywords:** MAX Phase, Composite, Squeeze casting, SHS synthesis, Pressure infiltration

## 1. Introduction

MAX type phases, so named in the 90s, are a relatively new material group of over 150 triple carbides or nitrides described by the general formula  $M_{n+1}AX_n$ , where M is an early transition metal, A is an element from group A (e.g. Al, Ga, In, Ge, Sn, Pb,

Si), X is carbon or nitrogen, and  $n=1-3$  [1-2]. MAX phases, also known as machinable ceramics, show a three-component layered molecular structure [3-4] and possess outstanding characteristics being a combination of the best features of ceramics and metals. They are known for their high thermal and electrical conductivity, high resistance to temperature variations, oxidation, abrasive wear and corrosion. They are also well machined using conventional



tools, have a high hardness and strength, which they maintain even at elevated temperatures.  $Ti_2AlC$ ,  $Ti_3AlC_2$  and  $Ti_3SiC_2$  are extensively described in the literature, as they are characterized by unique properties – the first two are lightweight and prone to oxidation, while the latter one, known since 1967, exhibits increased impact strength, energy absorption ability, high resistance to crack propagation and to changing of operating temperatures [5-7].

Among the reported studies, numerous examples of MAX phase-based composites manufacturing methods can be distinguished, which are gathered in Table 1. SHS is an efficient process of producing materials based on MAX phases, but as a rule it is linked to the development of porosity in the material, therefore, when manufacturing composite materials based on these phases, usually an additional infiltration process is required to obtain a solid and coherent material. One of the most common difficulties infiltrating porous preforms is the unsatisfactory degree of saturation of the preforms and the associated residual porosity. Even the newly published results related to aluminum matrix composites reinforced with  $Ti_2AlC$  or  $Ti_3AlC_2$  fabricated by HP [8], SPS [9] or ultrasonic agitation casting (a variant of stir casting) [10] indicate the same limitations. Due to the prolonged high-temperature treatment in [8-9], the in-situ formation of multiple Ti-Al inclusions was stated (e.g.  $Al_3Ti$ ,  $Al_4C_3$ ), disturbing the purity of the composite's chemical composition, while for the last technique [10], limitations such as density segregation and the tendency of the reinforcing particles to agglomerate occur. Additionally, the residual porosity and insufficient bonding at the matrix-reinforcement interface were observed [9]. These problems have been solved in the work of the Authors due to the use of the squeeze casting pressure infiltration method for the filling of spatial open-porous MAX phase preforms.

Table 1. Overview of manufacturing methods of composite materials reinforced with MAX phases (Ti-Al-C and Ti-Si-C) [8-26]

Ti-Al-C – based composites		Ti-Si-C – based composites	
Method	Material	Method	Material
Pressureless or current-activated pressure infiltration	$Ti_2AlC/TiC/Mg$ [11-12], $Ti_2AlC/Al$ [13]	SPS	$Ti_3SiC_2/Cu$ [18], $Ti_3SiC_2/WC-10Co$ [19], $Ti_3SiC_2/Cu/Al/SiC$ [20]
	In situ $Ti_3AlC_2/Al/TiC$ [14]		In situ $Ti_3SiC_2/TiSi_2$ [21]
VS	$Ti_3AlC_2/Al$ [15]	VS	$Ti_3SiC_2/Ni$ [22], $Ti_3SiC_2/Co$ , $Ti_3SiC_2/TiC$ [23], $Ti_3SiC_2/Al_2O_3$ [24], $Ti_3SiC_2/Ti$ , $Ti_3SiC_2/TiB_2$ [25]
HP	$Ti_2AlC/TiAl$ [16], $Ti_3AlC_2-Al_3Ti/Al$ [8]	HP	$Ti_3SiC_2/TiB_2$ , $Ti_3SiC_2/SiC$ , $Ti_3SiC_2/TiC_2$ [26]
SHS	$Ti_2AlC-Ti_3AlC_2/Al_2O_3$ , $Ti_2AlC/Al$ [17]		
SPS	$Ti_3AlC_2/Al$ [9]		
Ultrasonic agitation casting	$Ti_3AlC_2/Al$ [10]		

In this paper, dense, well-saturated Al-Si matrix composite materials reinforced with MAX phases from two systems (Ti-Al-C and Ti-Si-C) were manufactured with the use of two consecutive methods: Microwave Assisted Self-propagating High-temperature Synthesis (MASHS), used for the creation of open-porous MAX phase preforms, and squeeze casting pressure infiltration technique, utilized to impregnate them with the chosen Al alloy. The use of microwave radiation for the MASHS synthesis of the cellular MAX-type structures facilitates their production and makes it a cheaper and more efficient process in terms of time and energy than conventional methods like sintering. Moreover, the applied squeeze casting technique of infiltration secures the creation of dense and uniform composite material. Process parameters for both methods were tuned to assure the suitable porosity and to limit the possible chemical interactions between the composite's constituents. The microstructures and chemical compositions of the obtained materials were extensively elaborated. The reinforcement effects for both MAX phase systems were summarized in relation to mechanical (nanohardness, instrumental Young's modulus), wear (specific wear rate) and thermal (coefficient of thermal expansion) properties.

## 2. Materials and methods

Commercial powders of titanium (99% Ti, -325, Alfa Aesar), aluminum (99.9% Al, -325, Alfa Aesar), graphite (99.5% C, -325, SGL) and silicon carbide (99.8% SiC, 1  $\mu m$  or 44  $\mu m$ , Alfa Aesar) were used for the synthesis of MAX type phases in Ti-Al-C and Ti-Si-C systems. For a proper stoichiometric composition of substrates in both systems the following molar ratios of powders were prepared: Ti:Al:C – 2:1:1 and Ti:Si:C 3:1.2:1. An excess of Si was indispensable because of its tendency to evaporate during the SHS reaction. After weighing the ingredients to the nearest 0.001 g, the substrates were mixed for 10 minutes or subjected to the mechanical activation (MA) process in a ball mill for 3 h with ZrO<sub>2</sub> balls and BPR 10:1. Then, they were compacted by cold pressing with the use of uniaxial hydraulic press to obtain cylindrical samples with a diameter of 22 mm, while the pressing time at 930 MPa was 10 seconds for the Ti-Al-C system and 30-60 seconds for the Ti-Si-C system. Thus, prepared samples were subjected to MASHS, which was conducted in its “coupled mode” in the microwave reactor (Promis-Tech, Na Grobli St., Wroclaw, Poland, manufactured according to the guidelines of Prof. K. Naplocha) in the inert Ar atmosphere with a temperature recorded by Raytek Marathon MM (USA) pyrometer [27-28]. Such an approach was necessary because, in contrary to the sole Ti-Al-C system, the Ti-Si-C composition is not reactive enough to start the synthesis by itself. Ti-Si-C compact is hereby placed on the Ti-Al-C one and during the SHS synthesis of the first pellet, the second one is quickly heated up to the ignition point. Detailed synthesis routes and schemes were presented by the Authors elsewhere, a.o. [29-30]. Subsequently, manufactured porous preforms were subjected to squeeze casting pressure infiltration with a casting alloy EN AC-44200 (AC-AlSi12 (a)), belonging to the group of so-called eutectic silumins, which was chosen because of its high pourability. The chosen infiltration step parameters, after experimental selection and refinement, are given

as follows: 500-700°C – temperature of the preform, 200-300°C – temperature of the mold, 720-740°C – temperature of the Al-Si alloy during pouring, 90 MPa – compression pressure, 30-60 s – compression time. The structure observation and phase identification were performed by means of an optical microscope, JEOL JSM-6610A (Japan) and Hitachi S-3400N (Japan) scanning electron microscopes (SEM) and JEOL JED-2300 (Japan) and SwiftED3000 (UK) energy-dispersed X-ray spectrometers (EDS). To determine the volume percentage of reinforcement and matrix in the composite materials produced, Nikon NIS-Elements software was used. The samples were also analyzed in scanning (STEM) mode with the convergent beam with the use of Transmission Analytical Electron Microscopy (JEOL 2100 Electron Microscope with JEOL JED-2300 T EDS unit for the analytical measurements (Japan)). Spectra from XRD tests, described in details in [29-30], were subjected to quantitative analysis of the chemical composition by the Rietveld method to supplement the precise phase identification. Results of mechanical (nanohardness (HV), instrumental modulus of elasticity (EIT)), wear (abrasive wear resistance (WR)) and thermal (thermal expansion) properties tests were extensively discussed in [29-32], but are also summarized hereby to enable the comparison of the reinforcement effects. Tests of mechanical properties were carried out using the Oliver&Pharr method using the NHT nanohardness meter from Anton Paar (Austria) for the following parameters (indenter: diamond, Berkovich type, load: linear with a maximum of 50 mN, loading and unloading rate of 100 mN/min). Wear resistance investigations were performed using the "pin-on-flat" method in dry friction conditions with the reciprocating motion for various load values (0.1, 0.2 and 0.5 MPa), keeping other sliding parameters (distance of 2000 m, speed of 0.3 m/s, counter sample of CT70 tool steel) constant. The values of thermal expansion coefficients were determined in the temperature range of 50-500°C using a DIL 402 Netzsch dilatometer (Germany).

### 3. Results and discussion

#### 3.1. Microstructure, XRD and EDS analyses

In the materials produced during the initial preliminary pressure infiltration tests of the porous preforms (Fig. 1), the presence of undesirable oxide layers coating the inside of the porosity was observed. Their formation could be caused by too high temperature (equal to the one of the melted Al-Si alloy 720-740°C) and too long heating time of the reinforcement before infiltration. The chemical composition of these coatings is similar to titanium oxide (e.g. O - 69.384%, Ti - 25.376%, Al - 3.353%, Si - 1.887%). In subsequent tests, in order to avoid the effect of oxidation of the preform, its heating temperature was lowered to 500-700°C and the heating time was minimized.

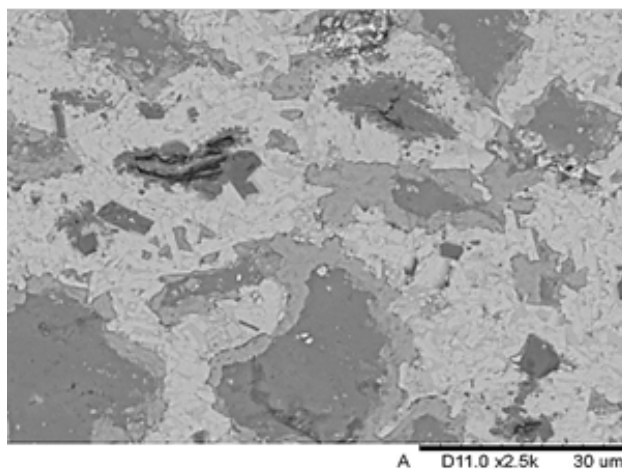


Fig. 1. View of the oxide layers (medium grey) covering the pores and separating the matrix phase (dark grey) from the MAX phase reinforcement (bright grey) after the infiltration process

The microstructures of composite materials produced after adjustment of process parameters of pressure infiltration with Al-Si alloy of open-porous preforms in Ti-Al-C (2a, 2b) and Ti-Si-C (2c, 2d) systems observed in optical microscopy are shown in Fig. 2. Liquid metal is forced to flow into the preform's cells, penetrating them and ensuring an almost thorough degree of saturation. The adapted squeeze casting process is so effective that it pressurizes the matrix material not only into the interior of pores but also between MAX type phase plate-like packages. In the Ti-Al-C system, MASHS synthesis produced porosities in the preforms are uneven in size but suitable to be infiltrated. Synthesized MAX phases have a characteristic nanolaminate structure composed of platelets, between which also some round inclusions were found that were further identified by EDS as TiC. Nevertheless, as the oriented texture of the material is not possible to be noticed due to the random arrangement of the platelets, the material's mechanical properties are expected to be isotropic [33]. The length of the  $Ti_2AlC$  plates is in the range of 10-30  $\mu m$ , while the finer ones of 5-10  $\mu m$  represent  $Ti_3AlC_2$ .  $Ti_2AlC$  and  $Ti_3AlC_2$  usually tend to exist side-by-side in the material, especially when the combustion temperature during SHS exceeds 1300°C [34]. In the case of materials based on Ti-Si-C system, the porosity of the preforms is much more regular and finer than in the Ti-Al-C one, which allows one to conclude that this material will be characterized by even greater uniformity of properties.  $Ti_3SiC_2$  phase consists of packages of elongated lamellar grains joined together (10-20  $\mu m$  in length, 1-3  $\mu m$  in thickness).

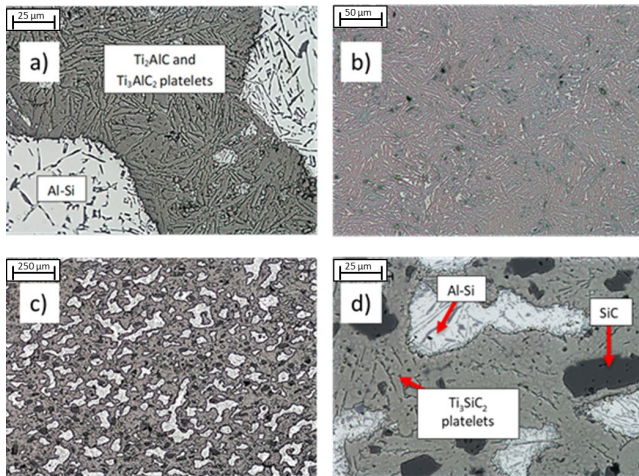


Fig. 2. Microstructures of composite materials manufactured on the matrix of Al-Si alloy reinforced with MAX phases: a), b) Al-Si + Ti-Al-C, c), d) Al-Si + Ti-Si-C

The microstructures of samples subjected to mechanical activation in the milling process were also investigated (Fig. 3). An increase in the reactivity of the powders was observed, facilitating the reaction and, consequently, causing a decrease in the synthesis temperature  $T_{comb}$ , which led to the creation of a material with a higher purity but with a greatly reduced degree of porosity. The materials produced in this way are almost solid, which excludes them from the possibility of application in research consistent with the purpose of the presented study. However, these results are promising for further work to produce MAX type condensed phases. Similar results were observed by Hashimoto et al. where for pretreatment in a planetary ball-mill, a greater degree of reactant homogenization was obtained than for mixing in a mortar, which resulted in a less porous product with greater homogeneity [35].

An exemplary map of the distribution of the elements, obtained during observation of the Al-Si+Ti-Al-C sample using a scanning electron microscope with the EDS function, shown in Fig. 4, confirms the co-occurrence of Al and Si in the matrix areas, as well as a uniform distribution of Ti, Al, C in the strengthening phase. In the matrix filling the interior porosity of the preform, no diffusion of elements from the reinforcing material was found. STEM line scan presented in Fig. 5 for the Al-Si+Ti-Si-C composite reveals a high concentration of Ti, Si, and C (bright area,  $Ti_3SiC_2$  platelets) arranged alternately with Al and Si elements (dark regions, EN AC-44200 matrix). Distinct, abrupt boundaries between these phases prove that no undesired chemical reactions took place during the infiltration of the preform with liquid metal.

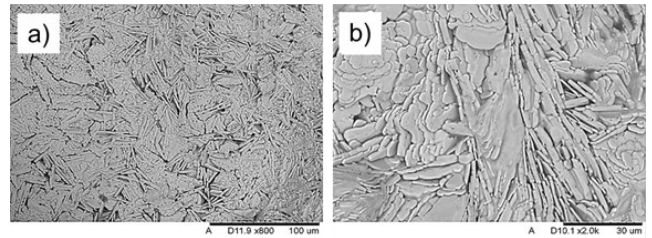


Fig. 3. Solid products of SHS synthesis after mechanical activation in the milling process (3h, BPR 10:1): a)  $Ti_2AlC$  and  $Ti_3AlC_2$  phases, b)  $Ti_3SiC_2$  phase

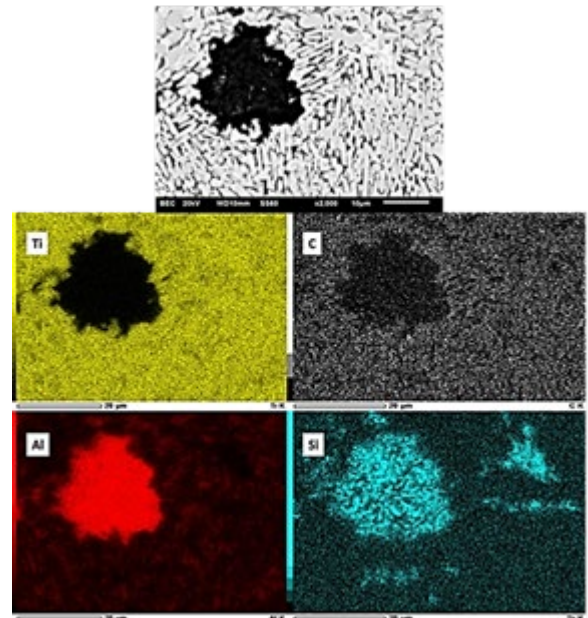


Fig. 4. Map of elements distribution for manufactured composite materials based on Al-Si alloy reinforced with MAX type ( $Ti_2AlC$  and  $Ti_3AlC_2$ ) phases

The obtained results of the volume content measurements conducted for matrix and reinforcement phases were averaged and the following values were obtained: 48.2% matrix and 51.8% reinforcement for the composite on the matrix of Al-Si alloy reinforced with  $Ti_2AlC/Ti_3AlC_2$  phases, and 39.6% of matrix and 60.4% reinforcement for the one strengthened with  $Ti_3SiC_2$  phase. It is assumed that the matrix content is consistent with the degree of open porosity of the MAX phase preforms produced.

Due to the large number of inclusions observed in a micro-scale in the composite materials, especially in the Ti-Si-C system, XRD tests of preforms were necessary to accurately identify their chemical composition [29-30]. The results for both systems are gathered in Table 2. In both cases, it was confirmed that the main component of the produced materials is the desired MAX phases. For the Ti-Al-C system, MAX phases ( $Ti_2AlC$  and  $Ti_3AlC_2$  in total) constitute 96.86%, while in the Ti-Si-C ( $Ti_3SiC_2$ ) system, it is 75.90% of the total material. However, in both systems, apart from the MAX phases, additional inclusions were also present: TiC for Ti-Al-C and TiC, SiC and  $TiSi_2$  for Ti-Si-C. Unlike some works, the synthesized products did not show inclusions of  $TiAl_3$ ,



Ti<sub>3</sub>Al, TiAl, TiAl<sub>2</sub>, Ti<sub>3</sub>AlC and Al<sub>2</sub>O<sub>3</sub> [36-37] in the Ti-Al-C system, or Ti<sub>5</sub>Si<sub>3</sub> in the Ti-Si-C system [38].

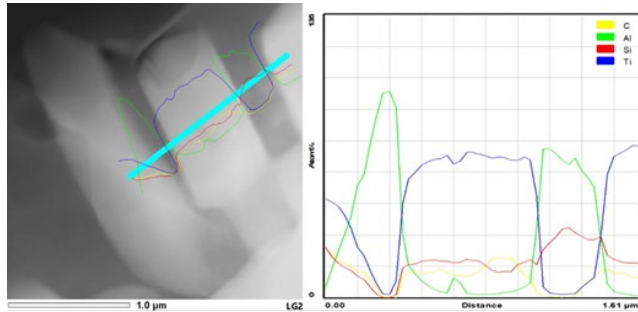


Fig. 5. STEM image at low-magnification and the EDS line profile showing the distribution profile of C, Al, Si and Ti elements along the cyan line (Ti<sub>3</sub>SiC<sub>2</sub> in Al-Si matrix)

Table 2. Results of quantitative chemical composition analysis of XRD spectra by the Rietveld method for manufactured preforms [29-30]

Ti-Al-C		Ti-Si-C	
Phase	Content [%]	Phase	Content [%]
Ti <sub>3</sub> AlC <sub>2</sub>	66.54	Ti <sub>3</sub> SiC <sub>2</sub>	75.90
Ti <sub>2</sub> AlC	30.32	TiC	14.71
TiC	3.14	TiSi <sub>2</sub>	8.27
		SiC	1.12

### 3.2. Evaluation of the reinforcement effect

Results of the tests of mechanical, thermal and wear properties, partially previously reported in [29-32], were summarized in Table 3, as a relative percentage ratio of each of the discussed properties of the composite materials reinforced with MAX type phases divided by the matrix parameters ( $\text{property}_{\text{composite}}/\text{property}_{\text{matrix}} \cdot 100\%$ ). In the case of wear resistance and thermal expansion coefficients the lower values indicate more beneficial and desired behavior.

The relative percentage change of HV and EIT for the composite materials in relation to the matrix parameters (Al-Si alloy, EN AC-44200, nanohardness - 159.8 HV and 1.6 GPa, Young's instrumental modulus - 29.0 GPa [29-30]) can be described as an approx. 4-fold increase in hardness and instrumental Young's modulus for Ti-Al-C system and more than 5-fold improvement in hardness and almost 6-fold in Young's modulus for Ti-Si-C one. The observed average improvement (for all loads) in abrasive wear resistance of the composite material compared to the matrix material is over two times for Al-Si+Ti-Al-C, while for Al-Si + Ti-Si-C it is about 20% (maximum reduction equaled 32% for 0.1 MPa load). The average specific wear rate of the matrix and Al-Si+Ti-Al-C or Al-Si+Ti-Si-C composites are respectively:  $3.5\text{-}4.8 \times 10^{-4} \text{ mm}^3/\text{Nm}$ ,  $1.6\text{-}2.3 \times 10^{-4} \text{ mm}^3/\text{Nm}$  and  $2.5\text{-}4 \times 10^{-4} \text{ mm}^3/\text{Nm}$ . Initially, up to 0.2 MPa, the specific wear rate rises with the load, but then it severely decreases with the load of 0.5 MPa, which coincides with the

observations described by other researchers [24] and can be explained by the fact that for higher load values, the matrix material, using its elasticity, additionally stabilizes the MAX phase platelets.

Table 3. Summary of the reinforcement effect for MAX phases of Ti-Al-C and Ti-Si-C systems in Al alloy matrix composite materials [29-32]

Material	Property	Property in relation to the one of the Al-Si matrix [%]
Ti <sub>2</sub> AlC/Ti <sub>3</sub> AlC <sub>2</sub> – composite	Nanohardness (HV)	368
Ti <sub>3</sub> SiC <sub>2</sub> – composite	Nanohardness (HV)	542
Ti <sub>2</sub> AlC/Ti <sub>3</sub> AlC <sub>2</sub> – composite	Instrumental Young's modulus (EIT)	408
Ti <sub>3</sub> SiC <sub>2</sub> – composite	Instrumental Young's modulus (EIT)	590
Ti <sub>2</sub> AlC/Ti <sub>3</sub> AlC <sub>2</sub> – composite	Specific wear rate (WR) for 0.1 MPa load	43
Ti <sub>3</sub> SiC <sub>2</sub> – composite	Specific wear rate (WR) for 0.1 MPa load	68
Ti <sub>2</sub> AlC/Ti <sub>3</sub> AlC <sub>2</sub> – composite	Specific wear rate (WR) for 0.2 MPa load	48
Ti <sub>3</sub> SiC <sub>2</sub> – composite	Specific wear rate (WR) for 0.2 MPa load	83
Ti <sub>2</sub> AlC/Ti <sub>3</sub> AlC <sub>2</sub> – composite	Specific wear rate (WR) for 0.5 MPa load	51
Ti <sub>3</sub> SiC <sub>2</sub> – composite	Specific wear rate (WR) for 0.5 MPa load	86
Ti <sub>2</sub> AlC/Ti <sub>3</sub> AlC <sub>2</sub> – composite	Coefficient of thermal expansion (CTE) at 50°C	57
Ti <sub>3</sub> SiC <sub>2</sub> – composite	Coefficient of thermal expansion (CTE) at 50°C	48
Ti <sub>2</sub> AlC/Ti <sub>3</sub> AlC <sub>2</sub> – composite	Coefficient of thermal expansion (CTE) at 100°C	59
Ti <sub>3</sub> SiC <sub>2</sub> – composite	Coefficient of thermal expansion (CTE) at 100°C	49
Ti <sub>2</sub> AlC/Ti <sub>3</sub> AlC <sub>2</sub> – composite	Coefficient of thermal expansion (CTE) at 200°C	66
Ti <sub>3</sub> SiC <sub>2</sub> – composite	Coefficient of thermal expansion (CTE) at 200°C	42
Ti <sub>2</sub> AlC/Ti <sub>3</sub> AlC <sub>2</sub> – composite	Coefficient of thermal expansion (CTE) at 300°C	63
Ti <sub>3</sub> SiC <sub>2</sub> – composite	Coefficient of thermal expansion (CTE) at 300°C	39
Ti <sub>2</sub> AlC/Ti <sub>3</sub> AlC <sub>2</sub> – composite	Coefficient of thermal expansion (CTE) at 400°C	49
Ti <sub>3</sub> SiC <sub>2</sub> – composite	Coefficient of thermal expansion (CTE) at 400°C	43
Ti <sub>2</sub> AlC/Ti <sub>3</sub> AlC <sub>2</sub> – composite	Coefficient of thermal expansion (CTE) at 500°C	38
Ti <sub>3</sub> SiC <sub>2</sub> – composite	Coefficient of thermal expansion (CTE) at 500°C	68

In addition, wear products from the composite material can create a tribofilm on the sample surface in the form of a protective oxide coating, limiting further deformation. For the Al-Si matrix sample, the wear mechanism is dominated by plastic deformation and grooving, common for metallic materials. MAX phases stiffen the matrix, preventing its plastic flow during the test. Moreover, many energy-absorbing processes delaying the wear effect, such as microcracks in the material or delamination between MAX-type plates also take place in the composite. It is assumed that because  $Ti_3SiC_2$  precipitates are smaller and easier to be extracted from the matrix the reinforcement effect for this system was less beneficial than for the Al-Si+Ti-Al-C one [23, 39].

The measured coefficients of thermal expansion confirm approx. two-fold average improvement in dimensional thermal stability of both produced composites compared to the matrix material. For the matrix material and Al-Si+Ti-Al-C composite, the expansion coefficient values show a slow upward trend and then, as the temperature continues to grow, they decrease up to the value of approx.  $7.3 \cdot 10^{-6} K^{-1}$ , while in the case of the Al-Si+Ti-Si-C composite, the coefficient of thermal expansion is almost constant as a function of temperature ( $8.5 \cdot 10^{-6} K^{-1}$ ). It can be concluded, comparing the above-mentioned results with the literature, that the temperature expansion of composite materials is comparable to the one of the MAX type phases, normally equaling  $5 \cdot 10^{-6} K^{-1}$  [40-44].

## 4. Conclusions

As was proved, it is possible to quickly and reproducibly manufacture MAX-type porous phases, both in Ti-Al-C and Ti-Si-C systems, by the MASHS method and subsequently to produce coherent composite materials reinforced with them by pressure infiltration. The main benefits provided by the microwave-assisted MAX phase synthesis lie in the shortening of their production process, lowering of its cost and energy consumption. In the Ti-Al-C system, the molar ratio of Ti:Al:C substrates suitable for obtaining a mixture of two MAX phases ( $Ti_2AlC$  and  $Ti_3AlC_2$ ) is 2:1:1, while in the Ti-Si-C system, it is necessary to use an excess of Si to obtain  $Ti_3SiC_2$ , with SiC as the source of Si. In this case, the molar ratio of Ti:Si:C powders is 3:1.2:1. The SHS synthesis for the Ti-Si-C system must be carried out in complex mode ("coupled SHS") together with a more reactive sample, which is a certain difficulty of the process. Porous preforms produced in the Ti-Al-C and Ti-Si-C systems are characterized by open porosity, that enables the successful pressure infiltration process. No additional adverse reactions between the matrix material and the preform resulting from the squeeze casting step were stated. The composite material did not show any additional phases, oxidation products, mutual diffusion between the matrix and reinforcement, or any other negative effects resulting from the liquid state pressing process. Preforms produced for selected molar ratios of substrates were characterized by high purity of chemical composition. However, in both systems, apart from the desired MAX phases, small amounts of inclusions were also present: Ti-Al-C:  $Ti_3AlC_2$ ,  $Ti_2AlC$  and TiC; Ti-Si-C:  $Ti_3SiC_2$ , TiC, SiC and  $TiSi_2$ . For the adopted process parameters of squeeze casting infiltration,

composite materials reinforced with MAX phase preforms produced in the MASHS process, were characterized by the following properties attributed to the strengthening effect:

- ✓ A high degree of infiltration of porosity (residual porosity only of several percent) with good adhesion between the composite's constituents,
- ✓ More than, respectively, two times and of a 20% lower average specific wear rate (for loads of 0.1, 0.2 and 0.5 MPa) for composite materials Al-Si+Ti-Al-C and Al-Si+Ti-Si-C, compared to the matrix material,
- ✓ Increased, compared to the matrix material, for composite materials Al-Si+Ti-Al-C and Al-Si+Ti-Si-C, respectively, hardness: by 368% and 542% and Young's modulus: by 408% and 590%,
- ✓ Approximately 2 times lower thermal expansion coefficient for composite materials Al-Si+Ti-Al-C and Al-Si+Ti-Si-C than the one for the Al-Si matrix.

## Acknowledgements

The Rietveld quantitative analysis of XRD tests results was carried out with the support of the KMM-VIN Research Fellowship, 01-30.11.2017. As for the STEM results, the authors acknowledge the CERIC-ERIC Consortium for the access to experimental facilities and financial support.

## References

- [1] Gonzalez-Julian, J. (2021). Processing of MAX phases: From synthesis to applications. *Journal of the American Ceramic Society*. 104, 659-690. <https://doi.org/10.1111/jace.17544>.
- [2] Barsoum, M.W. (2013). *MAX Phases: Properties of Machinable Ternary Carbides and Nitrides*. Wiley-VCH.
- [3] Arróyave, R., Talapatra, A., Duong, T., Son, W., Gao, H. & Radovic M. (2017). Does aluminum play well with others? Intrinsic Al-A alloying behavior in 211/312 MAX phases. *Materials Research Letters*. 5(3), 170-178. <https://doi.org/10.1080/21663831.2016.1241319>.
- [4] Khoptiar, Y. & Gotman, I. (2002).  $Ti_2AlC$  ternary carbide synthesized by thermal explosion, *Materials Letters*. 57(1), 72-76. [https://doi.org/10.1016/S0167-577X\(02\)00701-2](https://doi.org/10.1016/S0167-577X(02)00701-2).
- [5] Jeitschko, W. & Nowotny, H. (1967). Die kristallstruktur von  $Ti_3SiC_2$ -ein neuer komplexcarbidge-typ. *Monatshefte Für Chemie*. 98, 329-337. <https://doi.org/10.1007/BF00899949>.
- [6] El Saeed, M.A., Deorsola, F.A. & Rashad, R.M. (2013). Influence of SPS parameters on the density and mechanical properties of sintered  $Ti_3SiC_2$  powders. *International Journal of Refractory Metals and Hard Materials*. 41, 48-53. <https://doi.org/10.1016/j.ijrmhm.2013.01.016>.
- [7] Radhakrishnan, R., Williams, J.J. & Akinc M. (1999). Synthesis and high-temperature stability of  $Ti_3SiC_2$ . *Journal of Alloys and Compounds*. 285(1-2), 85-88. [https://doi.org/10.1016/S0925-8388\(99\)00003-1](https://doi.org/10.1016/S0925-8388(99)00003-1).
- [8] Wang, Y., Huang, Z., Hu, W., Cai, L., Lei, C., Yu, Q. & Jiao Y. (2021). Preparation and characteristics of  $Ti_3AlC_2$ -

- Al<sub>3</sub>Ti/Al composite materials synthesized from pure Al and Ti<sub>3</sub>AlC<sub>2</sub> powders. *Materials Characterization*. 178, 111298. <https://doi.org/10.1016/j.matchar.2021.111298>.
- [9] Wang, Z., Ma, Y., Sun, K., Zhang, Q., Zhou, C., Shao, P., Xiu, Z. & Wu, G. (2022). Enhanced ductility of Ti<sub>3</sub>AlC<sub>2</sub> particles reinforced pure aluminum composites by interface control. *Materials Science and Engineering: A*. 832, 142393. <https://doi.org/10.1016/j.msea.2021.142393>.
- [10] Zhai, W., Pu, B., Sun, L., Xu, L., Wang, Y., He, L., Dong, H., Gao, Y., Han, M. & Xue, Y. (2022). Influence of Ti<sub>3</sub>AlC<sub>2</sub> content and load on the tribological behaviors of Ti<sub>3</sub>AlC<sub>2</sub>p/Al composites. *Ceramics International*. 48(2), 1745-1756. <https://doi.org/10.1016/j.ceramint.2021.09.254>.
- [11] Anasori, B., Caspi, E.N. & Barsoum, M.W. (2014). Fabrication and mechanical properties of pressureless melt infiltrated magnesium alloy composites reinforced with TiC and Ti<sub>2</sub>AlC particles. *Materials Science and Engineering: A*. 618, 511-522. <https://doi.org/10.1016/j.msea.2014.09.039>.
- [12] Anasori, B. & Barsoum, M.W. (2016). Energy damping in magnesium alloy composites reinforced with TiC or Ti<sub>2</sub>AlC particles. *Materials Science and Engineering: A*. 653, 53-62. <https://doi.org/10.1016/j.msea.2015.11.070>.
- [13] Hu, L., Kothalkar, A., O'Neil, M., Karaman, I. & Radovic, M. (2014). Current-activated, pressure-assisted infiltration: A novel, versatile route for producing interpenetrating ceramic-metal composites. *Materials Research Letters*. 2, 124-130. <https://doi.org/10.1080/21663831.2013.873498>.
- [14] Song, I.H., Kim, D.K., Hahn, Y.D. & Kim, H.D. (2004). Investigation of Ti<sub>3</sub>AlC<sub>2</sub> in the in situ TiC-Al composite prepared by the exothermic reaction process in liquid aluminum. *Materials Letters*. 58(5), 593-597. [https://doi.org/10.1016/S0167-577X\(03\)00576-7](https://doi.org/10.1016/S0167-577X(03)00576-7).
- [15] Wang, W.J., Gauthier-Brunet, V., Bei, G.P., Laplanche, G., Bonneville, J., Joulain, A. & Dubois, S. (2011). Powder metallurgy processing and compressive properties of Ti<sub>3</sub>AlC<sub>2</sub>/Al composites. *Materials Science and Engineering: A*. 530, 168-173. <https://doi.org/10.1016/j.msea.2011.09.068>.
- [16] Chen, Y.L., Yan, M., Sun, Y.M., Mei, B.C. & Zhu, J.Q. (2009). The phase transformation and microstructure of TiAl/Ti<sub>2</sub>AlC composites caused by hot pressing. *Ceramics International*. 35(5), 1807-1812. <https://doi.org/10.1016/j.ceramint.2008.10.009>.
- [17] Fedotov, A.F., Amosov, A.P., Latukhin, E.I. & Novikov, V.A. (2016). Fabrication of aluminum-ceramic skeleton composites based on the Ti<sub>2</sub>AlC MAX phase by SHS compaction. *Russian Journal of Non-Ferrous Metals*. 57(5), 33-40. <https://doi.org/10.3103/S1067821216010053>.
- [18] Dang, W., Ren, S., Zhou, J., Yu, Y., Li, Z. & Wang, L. (2016). Influence of Cu on the mechanical and tribological properties of Ti<sub>3</sub>SiC<sub>2</sub>. *Ceramics International*. 42(8), 9972-9980. <https://doi.org/10.1016/j.ceramint.2016.03.099>.
- [19] Shi, X., Wang, M., Xu, Z., Zhai, W. & Zhang, Q. (2013). Tribological behavior of Ti<sub>3</sub>SiC<sub>2</sub>/(WC-10Co) composites prepared by spark plasma sintering. *Materials & Design*. 45, 365-376. <https://doi.org/10.1016/j.matdes.2012.08.069>.
- [20] Dang, W., Ren, S., Zhou, J., Yu, Y. & Wang, L. (2016). The tribological properties of Ti<sub>3</sub>SiC<sub>2</sub>/Cu/Al/SiC composite at elevated temperatures. *Tribology International*. 104, 294-302. <https://doi.org/10.1016/j.triboint.2016.09.008>.
- [21] Krinitcyn, M., Fu, Z., Harris, J., Kostikov, K., Pribytkov, G.A., Greil, P. & Travitzky, N. (2017). Laminated object manufacturing of in-situ synthesized MAX-phase composites. *Ceramics International*. 43(12), 9241-9245. <https://doi.org/10.1016/j.ceramint.2017.04.079>.
- [22] Li, H., Peng, L.M., Gong, M., He, L.H., Zhao, J.H. & Zhang, Y.F. (2005). Processing and microstructure of Ti<sub>3</sub>SiC<sub>2</sub> / M (M = Ni or Co) composites. *Materials Letters*. 59(21), 2647-2649. <https://doi.org/10.1016/j.matlet.2005.04.010>.
- [23] Sun, Z., Zhou, M.C. & Li, S. (2002). Tribological behavior of Ti<sub>3</sub>SiC<sub>2</sub> based materials. *Journal of Materials Science & Technology*. 18(2), 142-145.
- [24] Hu, C., Zhou, Y., Bao, Y. & Wan, D. (2006). Tribological properties of polycrystalline Ti<sub>3</sub>SiC<sub>2</sub> and Al<sub>2</sub>O<sub>3</sub>-reinforced Ti<sub>3</sub>SiC<sub>2</sub> composites. *Journal of the American Ceramic Society*. 89(11), 3456-3461. <https://doi.org/10.1111/j.1551-2916.2006.01253.x>.
- [25] Yang, J., Gu, W., Pan, L.M., Song, K., Chen, X. & Qiu, T. (2011). Friction and wear properties of in situ (TiB<sub>2</sub>+TiC)/Ti<sub>3</sub>SiC<sub>2</sub> composites. *Wear*. 271(11-12), 2940-2946. <https://doi.org/10.1016/j.wear.2011.06.017>.
- [26] Lis, J., Chlubny, L., Łopaciński, M., Stobierski, L. & Bućko, M.M. (2008). Ceramic nanolaminates-Processing and application. *Journal of the European Ceramic Society*. 28(5), 1009-1014. <https://doi.org/10.1016/j.jeurceramsoc.2007.09.033>.
- [27] Naplocha, K. (2013). *Composite materials strengthened with preforms produced in the process of high-temperature synthesis in a microwave field (in Polish: Materiały kompozytowe umacniane preformami wytworzonymi w procesie wysokotemperaturowej syntezy w polu mikrofalowym)*. Wrocław: Oficyna Wydawnicza PWR.
- [28] Merzhanov, G. (2011). Thermally coupled SHS reactions. *International Journal of Self-Propagating High-Temperature Synthesis*. 20, 61-63. <https://doi.org/10.3103/S1061386211010109>.
- [29] Dmitruk, A., Żak, A., Naplocha, K., Dudziński, W. & Morgiel, J. (2018). Development of pore-free Ti-Al-C MAX/Al-Si MMC composite materials manufactured by squeeze casting infiltration. *Materials Characterization*. 146, 182-188. <https://doi.org/10.1016/j.matchar.2018.10.005>.
- [30] Dmitruk, A., Naplocha, K., Żak, A., Strojny-Nędza, A., Dieringa, H. & Kainer K.U. (2019). Development of pore-free Ti-Si-C MAX/Al-Si composite materials manufactured by squeeze casting infiltration. *Journal of Materials Engineering and Performance*. 28, 6248-6257. <https://doi.org/10.1007/s11665-019-04390-8>.
- [31] Dmitruk, A., Naplocha, K. & Strojny-Nędza, A. (2018). Thermal properties of Al alloy matrix composites reinforced with MAX type phases. *Composites Theory and Practice*. 18(1), 32-36.
- [32] Dmitruk, A. & Naplocha, K. (2018). Manufacturing of Al alloy matrix composite materials reinforced with MAX phases. *Archives of Foundry Engineering*. 18(2), 198-202. DOI: 10.24425/122528.
- [33] Chen X. & Bei G. (2017). Toughening mechanisms in nanolayered MAX phase ceramics-a review. *Materials (Basel)*. 10(4), 1-12. <https://doi.org/10.3390/ma10040366>.

- [34] Yang, J., Liao, C., Wang, J., Jiang, Y. & He, Y. (2014). Effects of the Al content on pore structures of porous Ti<sub>3</sub>AlC<sub>2</sub> ceramics by reactive synthesis. *Ceramics International*. 40(3), 4643-4648. <https://doi.org/10.1016/j.ceramint.2013.09.004>.
- [35] Hashimoto, S., Nishina, N., Hirao, K., Zhou, Y., Hyuga, H., Honda, S. & Iwamoto, Y. (2012). Formation mechanism of Ti<sub>2</sub>AlC under the self-propagating high-temperature synthesis (SHS) mode. *Materials Research Bulletin*. 47(5), 1162-1168. <https://doi.org/10.1016/j.materresbull.2012.02.003>.
- [36] Yang, J., Liao, C., Wang, J., Jiang, Y. & He, Y. (2014). Reactive synthesis for porous Ti<sub>3</sub>AlC<sub>2</sub> ceramics through TiH<sub>2</sub>, Al and graphite powders. *Ceramics International*. 40(5), 6739-6745. <https://doi.org/10.1016/j.ceramint.2013.11.136>.
- [37] Hendaoui, A., Vrel, D., Amara, A., Langlois, P., Andasmas, M. & Guerioune, M. (2010). Synthesis of high-purity polycrystalline MAX phases in Ti-Al-C system through mechanically activated self-propagating high-temperature synthesis. *Journal of the European Ceramic Society*. 30(4), 1049-1057. <https://doi.org/10.1016/j.jeurceramsoc.2009.10.001>.
- [38] Yeh, C.L. & Shen, Y.G. (2008). Effects of SiC addition on formation of Ti<sub>3</sub>SiC<sub>2</sub> by self-propagating high-temperature synthesis. *Journal of Alloys and Compounds*. 461(1-2), 654-660. <https://doi.org/10.1016/j.jallcom.2007.07.088>.
- [39] Zhang, Y., Ding, G.P., Zhou, Y.C. & Cai, B.C. (2002). Ti<sub>3</sub>SiC<sub>2</sub> - a self-lubricating ceramic, *Materials Letters*. 55(5), 285-289. [https://doi.org/10.1016/S0167-577X\(02\)00379-8](https://doi.org/10.1016/S0167-577X(02)00379-8).
- [40] Radovic, M. & Barsoum, M.W. (2013). MAX phases: Bridging the gap between metals and ceramics. *American Ceramic Society Bulletin*. 92(3), 20-27.
- [41] Barsoum, M.W., El-raghy, T., Rawn, C.J., Porter, W.D., Wang, H., Payzant, E.A. & Hubbard, C.R. (1999). Thermal properties of Ti<sub>3</sub>SiC<sub>2</sub>. *Journal of Physics and Chemistry of Solids*. 60(4), 429-439. [https://doi.org/10.1016/S0022-3697\(98\)00313-8](https://doi.org/10.1016/S0022-3697(98)00313-8).
- [42] Son, W., Duong, T., Talapatra, A., Gao, H., Arróyave, R. & Radovic, M. (2016). Ab-initio investigation of the finite-temperatures structural, elastic, and thermodynamic properties of Ti<sub>3</sub>AlC<sub>2</sub> and Ti<sub>3</sub>SiC<sub>2</sub>. *Computational Materials Science*. 124, 420-427. <https://doi.org/10.1016/j.commatsci.2016.08.015>.
- [43] Shih, C., Meisner, R., Porter, W., Katoh, Y. & Zinkle, S.J. (2013). Physical and thermal mechanical characterization of non-irradiated MAX phase materials (Ti-Si-C and Ti-Al-C systems). *Fusion Reactor Materials Program*. 55, 78-93.
- [44] Wang, X.H. & Zhou, Y.C. (2010). Layered Machinable and electrically conductive Ti<sub>2</sub>AlC and Ti<sub>3</sub>AlC<sub>2</sub> ceramics: a review. *Journal of Materials Science & Technology*. 26(5), 385-416. [https://doi.org/10.1016/S1005-0302\(10\)60064-3](https://doi.org/10.1016/S1005-0302(10)60064-3).